Short-wave Infrared Neural Stimulation Drives Graded Sciatic Nerve Activation Across A Continuum of Wavelengths

Brandon S. Coventry *Student Member, IEEE*, Justin T. Sick, Thomas M. Talavage *Member, IEEE*, Keith M. Stantz, and Edward L. Bartlett ¥

***Abstract*— Infrared neural stimulation (INS) is an optical stimulation technique which uses coherent light to stimulate nerves and neurons and which shows increased spatial selectivity compared to electrical stimulation. This could improve deep brain, high channel count, or vagus nerve stimulation. In this study, we seek to understand the wavelength dependence of INS in the near-infrared optical window. Rat sciatic nerves were excised *ex vivo* and stimulated with wavelengths between 700 and 900 nm. Recorded compound nerve action potentials (CNAPs) showed that stimulation was maximized in the 700 nm window despite comparable laser power levels across wavelengths. Computational models demonstrated that wavelength-based activation dependencies were not a result of passive optical properties. This data demonstrates that INS is both wavelength and power level dependent, which inform stimulation systems to actively target neural microcircuits in humans.**

I. Introduction

Despite the clinical success of neuromodulation-based therapeutics such as deep brain and vagus nerve stimulators and the cochlear implant, their efficacy is limited by large scale activation[1–3] and current spillover [1] implicit to electrical stimulation modalities. This nonspecific activation causes aberrant auditory percepts in cochlear implants and adverse perceptual side effects in deep brain and vagus nerve stimulators[4]. While novel methods of current stearing arrays can limit current spread, models of current steering still show field strengths that can extend into the millimeter range [5], [6]. Furthermore, electrical stimulation of the nervous system can drive cytotoxic levels of reactive oxygen species[7] and the necessity to be in direct contact with tissue can drive tissue death[8].

Infrared neural stimulation (INS) is an optical stimulation technique which utilizes coherent infrared light to selectively stimulate nerves and neurons[9]. INS is advantageous over electrical stimulation because it has demonstrated better spatial selectivity[2,10] ,does not need to be in direct contact with tissue[9], and can be performed safely over long periods of time[11]. Furthermore, unlike other methods such as optogenetics[12], INS does not require genetic modification. While full safety trials have not yet been performed, studies in chronically implanted cats suggests long-term safety and stability of INS optrodes can be achieved [13].

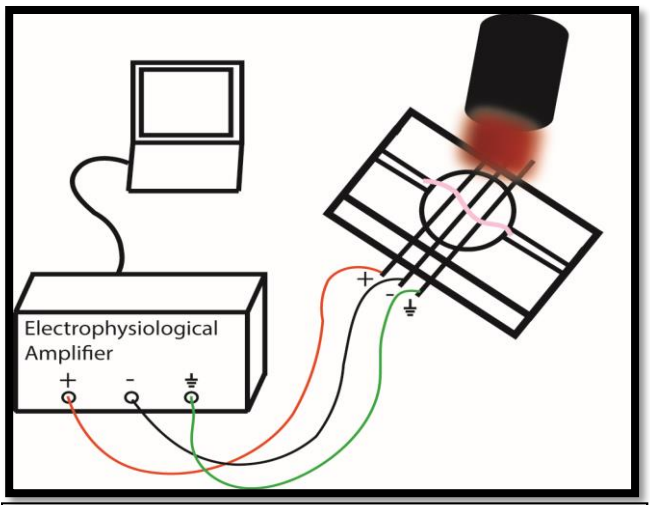

Fig 1. Schematic of the experimental prep. CNAPs were recorded from sciatic nerves differentially in response to free-field application of 700-900 nm infrared light.

Despite INS advantages over electrical stimulation, the mechanisms of infrared activation remain elusive and thus limit development. Previous studies have suggested that optimal wavelengths for stimulation lie largely in the mid-infrared range (1800-2000 nm), correlating to peaks in the water absorption spectrum[11]. It has been suggested that this absorption can drive the generation of heat which in turn stimulates nerves and neurons[14,15]. Furthermore, with careful control of laser parameters, heat spread has been hypothesized to be controlled in a thermal confinement regime[16]. However, this hypothesis becomes less plausible with studies using UV[17] and near-IR[18] wavelengths for activation where absorption is highly attenuated compared to longer wavelengths.

A second mechanistic question is whether activation scales with choice of wavelength, a photoelectric-like effect[19], or

*Research supported by the National Institutes of Health NIDCD DC011580. ¥ Corresponding Author

B. S. Coventry is with the Weldon School of Biomedical Engineering, Purdue University West Lafayette, IN 47907 USA.

J. T. Sick was with the School of Health Sciences, Purdue University, West Lafayette, IN 47907,USA. Dr. Sick is now with the Mary Bird Perkins Cancer Center, Baton Rouge, LA USA.

T. M. Talavage is with the Weldon School of Biomedical Engineering and the School of Electrical and Computer Engineering, Purdue University, West Lafayette, IN, USA

K. M. Stantz is with the School of Health Sciences, Purdue University, West Lafayette, IN 47907 USA and the Department of Radiology and Imaging Sciences, Indiana University School of Medicine, Indianapolis IN 46202, USA.

E. L. Bartlett ¥ is with the School of Biological Sciences and the Weldon Schoolf of Biomedical Engineering, Purdue University, West Lafayette, IN 47907, USA. phone: (765) 496-1425; e-mail: ebartle@purdue.edu

the power of laser stimulation. Previous studies of INS have focused on single-wavelength systems, leaving wavelength-activation level functions unstudied. If activation of tissue is photoelectric in nature as suggested in previous studies, then activation should be highly dependent on choice of wavelength and insensitive to optical power output. The objective of this study is to categorize INS activation of the sciatic nerve across a range of near-infrared wavelengths. Furthermore, we aim to test whether measurement are consistent with water absorption as the primary causative mechanism for INS.

II. Methods

A. Surgical Preparation

All surgical procedures were performed in accordance with the Purdue University animal care and use committee (PACUC 06-106). Fisher-344 rats of either sex were deeply anesthetized by induction of isofluorane followed by an overdose of Beuthanasia (200 mg/kg). After loss of toe-pinch and righting-reflex autonomic function, rats underwent transcardiac perfusion with phosphate buffered saline (PBS). Sciatic nerves were surgically extracted by making an incision down midline of the biceps femoris muscle of each leg until the sciatic nerve was visible[20]. Sciatic nerve processes from proximal to the L4-L5 spinal root to the greater trochanter a septum were excised and rapidly placed into oxygenated artificial cerebrospinal fluid (ACSF) [Paul and Cox]. Sciatic nerves were kept in ACSF oxygenated with 95% O_2/5% CO_2 until placed in the lasing setup.

B. IR Laser System and Electrophysiological Recordings

Sciatic nerves were placed into a custom-made bath and electrode housing for differential recording of compound nerve action potentials (CNAPs). A total of 3 rats were utilized for this study with a total of 25,674 CNAPs recorded. The experimental setup is illustrated in Fig 1. Nerves were placed on 3 silver/silver-chloride recording electrodes with individual electrodes designated as positive, negative, or ground. Nerves and electrodes were submerged in oxygenated ACSF to ensure nerve health. Differential CNAP recordings were acquired and discretized utilizing an ISODAMA8 amplifier (WPI) and recorded in LabScribe software (V4, iWorx). Sampling rates for collection of CNAPs was set to 10kHz.

Laser stimuli were generated using a Q10 quantel Q-smart Rainbow optical parametric oscillator system. Wavelengths were varied between 700-900 nm. Repetition rate and pulse width were fixed at 10 Hz and 10 ns, respectively. Optical irradiation was delivered to the nerve bath free-field from an optical fibre ~10cm above the nerve. Average power levels were measured after each experiment with an optical power meter, with minimum measured powers of 0 mW and maximum measured average power level of 14.05 mW. Utilizing Jacques model, we found that laser stimuli lay squarely in both thermal and pressure confined regions[16].

C. Data Analysis

Data were exported from LabScribe to Matlab for analysis. CNAPs were detected using a threshold-match filtering technique. Samples of CNAPs were randomly sampled and detected when surpassing 3 standard deviations from mean threshold. Sampled responses were then used to form a template for matched filter detection. As laser powers were not consistent between nerves, optical powers were measured after each stimulation period and binned into 4 equal sized power bins of 0-4, 4-8, 8-12, and >12 mW power levels for statistical comparison.

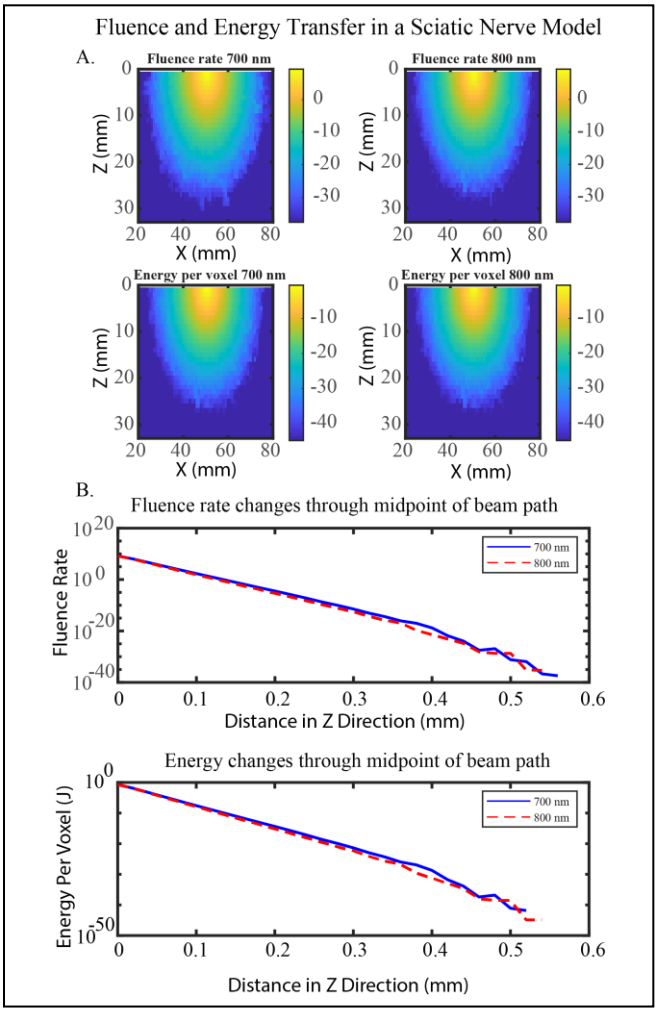

Fig 2: Computational modeling of Fluence rate and energy deposition from 700 and 800 nm excitation in the sciatic nerve (A). Slicing the model through the centroid of the beam path reveals that fluence rate and energy per pixel shows no difference in wavelength.

Statistical analysis was done using a two-way ANOVA with multiple comparisons correction via Tukey's honest significant difference method. Data outliers were detected via the quartile method, in which data more than 1.5 interquartile ranges above the upper quartile or below the lower quartile. All statistical analyses were performed in Matlab software.

D. Modeling of Light-Nerve interactions

Modeling of tissue absorption and scattering was performed using Monte-Carlo simulations implemented with

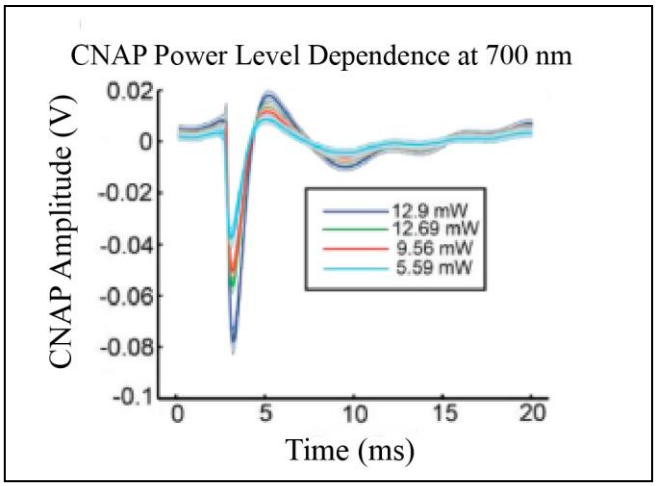

Fig 3. Sciatic nerve CNAP responses elicited from a 700 nm laser source. Responses are graded with respect to laser power level.

MCX Lab[21] software with visualization in Matlab (Mathworks). Sciatic nerve absorption, scattering, and anisotropy coefficients from myelinated and unmyelinated were obtained from previous optical parameter studies and were used as inputs to the model[22, 23].

Simulations consisted of $1 * 10^8$ photons sampled via Monte-Carlo methods which estimates the fractional density matrix of tissue absorption $\left[\frac{1}{cm^3}\right]$ in response to one packet of energy delivered via photon. The radiant energy density matrix can then be derived by scaling the fractional density matrix of absorption by the delivered energy of the optical source. Optical fluence is then derived by observing photon upper and lower boundary egress and converting absorbance to a transport matrix by parameterizing absorbance into cylindrical coordinates and scaling by delivered energy of the optical source[21, 24].

Wavelength dependent properties are listed in table 1. Scattering coefficients were empirically determined following Jacques' et al. modeling[22]:

$$\mu_s(\lambda) = a\left(f_{Ray}\left(\frac{\lambda}{500}\right)^{-4} + (1 - f_{Ray})\left(\frac{\lambda}{500}\right)^{-b}\right)$$

where af_{Ray} is the Rayleigh scattering component and $(1 - f_{Ray})\left(\frac{\lambda}{500}\right)^{-b}$ is the Mie scattering component.

Table I: Coefficients for optical fluence model

Wavelength	a	b	f_{Ray}	μ_a	μ_s
700	25.9	1.1560	0	1.25	17.5540
800	25.9	1.1560	0	1.5	15.0431

The sciatic nerve was modeled as a cubic slice of white matter with 100 pixels in each dimension. Individual pixel volume was set to 200 μm with a 2mm x 2mm x 2mm size nerve, in agreement with anatomical studies. The optic source consisted of a Gaussian beam shape radiating from a 200 μm diameter fiber, similar to our laser setup, with optical sensors placed on all corners of the simulation space. Time-domain simulations were done over a 10 ns interval corresponding to *ex vivo* laser pulse-widths with a sampling interval of $1 * 10^{-10}$ s.

III. Results

In this study, we elicited CNAP responses from sciatic nerve utilizing near IR stimuli across the continuum of 700 and 900 nm. Furthermore, computational models of tissue fluence and energy absorption were developed to assess nerve activation in response to optical energy absorption.

A. Computational modeling shows no difference in energy absorption across stimulation wavelengths

A computational model of the passive optical processes of the sciatic nerve was generated using MCXLab software. We hypothesized that fluence rates will dictate tissue absorption and can be used to predict CNAP levels in the sciatic nerve. Monte-Carlo optical simulations show that optical fluence and energy have similar spatial spreads between 700 and 800 nm (Fig 2A). Furthermore, examining fluence rates and energy per pixel through the optical center of the beam path, representing maximal activation, reveals that energy deposition remains approximately equal between 700 and 800 nm simulations (Fig 2B). This suggests that heat generation and its spatial spread should be nearly identical. Therefore, any wavelength or stimulation level dependence is not a function of heat generation or passive optical properties of the nerve itself.

B. Near-IR activation of sciatic nerve shows graded power level CNAP responses.

Our next goal was to assess the role of optical intensity across the continuum of near-infrared wavelengths in INS activation of the sciatic nerve. At a fixed wavelength of 700 nm, a clear intensity dependence can be seen (Figure 3A) which is consistent across 1500 trials (Figure 3B). This intensity dependence suggests that the underlying mechanism does not follow a photoelectric type effect which is independent of intensity effects.

Next, we explored the interplay of intensity and wavelength in INS activation. Interestingly, with the exception of 700 nm, responses stayed relatively consistent across power levels and wavelength (Fig 3, 4). Varying near-IR wavelengths revealed clear CNAP activation profiles with unique optical power level dependencies. A two-way ANOVA showed statistical differences ($p<0.05$) between 700 nm and 750, 800, 850, and 900 nm wavelengths at all binned power levels. Furthermore, at each power bin, only 750, 800, and 850 nm at the lowest power bin, 750 and 900 nm at 4-8 mW, and 800 and 900 nm at 8-12 mW showed no significant difference in peak to peak amplitudes ($p>0.05$). These unique activation profiles are likely from intrinsic excitation and absorption properties of the nerve and its molecular composition, as model results suggest energy depositions were roughly equivalent between 700 and 800 nm (Fig 2) and thus can not account for marked increases in CNAP activation across wavelengths.

IV. Discussion

In this study, we demonstrate that INS is not limited to a fixed number of specific wavelengths near the water absorption peak, as suggested by previous studies[11] but

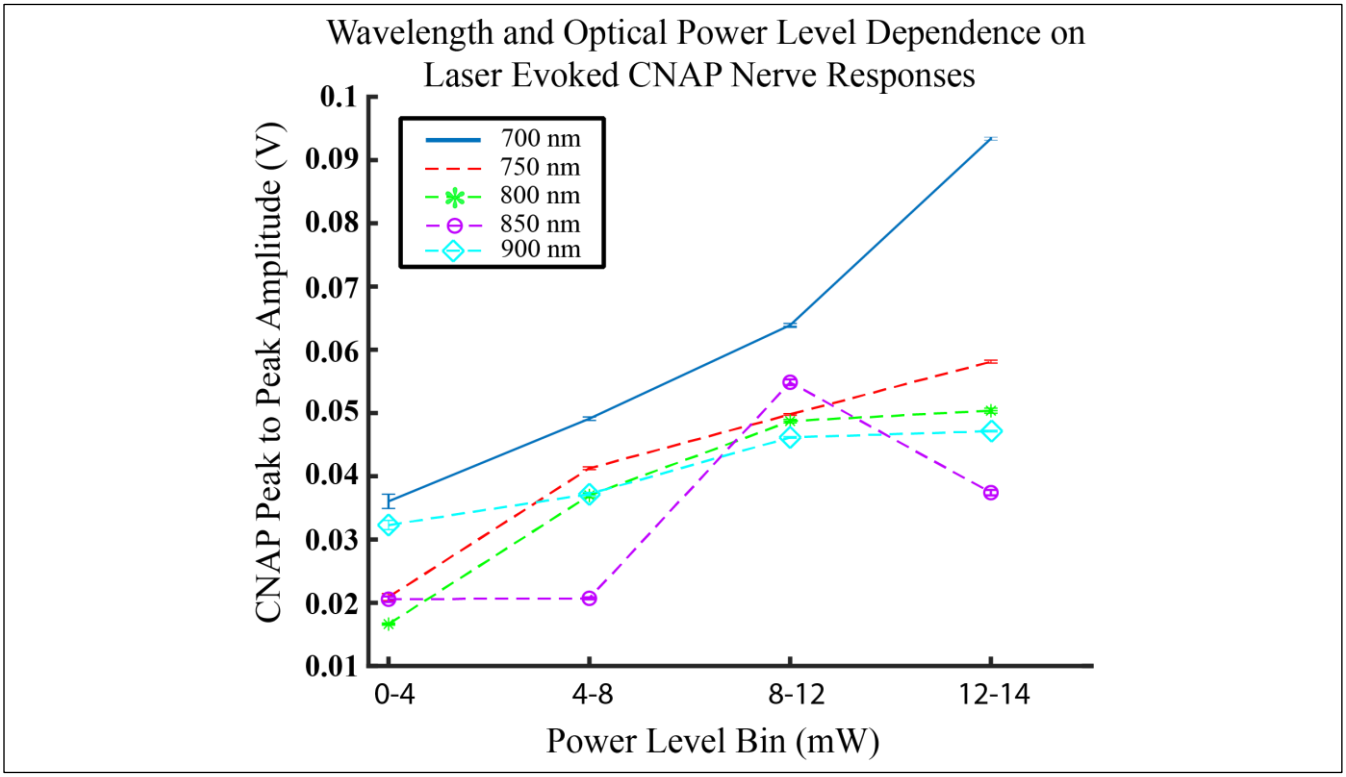

Fig 4. Wavelength and optical power level dependence on sciatic nerve evoked responses. Varying wavelengths elicit different CNAP activation profiles.

exist across the continuum of the infrared spectrum. There are a few possible explanations for activation driven by near-infrared wavelengths. First, there may be a specialized chromophore within the neuron acting as an energy transducer. Mitochondria are known to contain various chromophores[25] and are involved in generation of intracellular calcium waves correlated with IR stimulation[26]. Another possibility is absorption mediated by a heme group, which would dominate activation near 700 nm with decreased activation as wavelength redshifts [27].

Second, the majority of previous INS studies have been conducted using wavelengths and pulse-widths squarely in thermal confinement[28], where rapid heat gradients are the main energy producer[16]. However, assuming the speed of sound and thermal diffusivity through ACSF is roughly that of salt water (~1520 m/s, 0.143 ∗10−6 m2/s respectively), then our laser-tissue system is acting in both thermal and pressure confinement regimes[16], demonstrating that high locally confined pressure gradients can drive stimulation similar to localized temperature gradients. Other studies have also posited that optical activation may be driven by the photoelectric effect [19]. However, the data shown here refute this claim as photoelectric effects are functions of optical wavelengths and not intensities.

V. Conclusion

In this study, we demonstrated that infrared neural stimulation is not limited to a subset of optical windows, but across the continuum of near infrared wavelengths. Further, we demonstrate that optical stimuli at different wavelengths with similar radiant energies can evoke different activation profiles. This then suggests that laser stimuli can be fine-tuned to create specialized activation profiles for stimulation-based therapeutics.

Acknowledgment

The authors thank Alexandra Sommer and Jessica Page for their assistance with surgical procedures and transportation of samples to the laser preparation.

References

[1] M. Noor, K. Murari, C. McCracken, and Z. Kiss, “Spatiotemporal dynamics of cortical perfusion in response to thalamic deep brain stimulation,” *Neuroimage*, vol. 126, pp. 131–139, 2016.

[2] A. D. Izzo, E. Suh, J. Pathria, J. T. Walsh, D. S. Whitlon, and C.-P. Richter, “Selectivity of neural stimulation in the auditory system: a comparison of optic and electric stimuli.,” *J. Biomed. Opt.*, vol. 12, no. 2, p. 021008, 2007.

[3] J. B. Ranck, “Which elements are excited in electrical stimulation of mammalian central nervous system: a review,” *Brain Res.*, vol. 98, no. 3, pp. 417–440, 1975.

[4] H. Cagnan, T. Denison, C. McIntyre, and P. Brown, “Emerging technologies for improved deep brain stimulation,” *Nat. Biotechnol.*, vol. 37, no. 9, pp. 1024–1033, 2019.

[5] P. Reker, T. A. Dembek, J. Becker, V. Visser-Vandewalle, and L. Timmermann, "Directional deep brain stimulation: A case of avoiding dysarthria with bipolar directional current steering," *Park. Relat. Disord.*, vol. 31, pp. 156–158, 2016.

[6] C. R. Butson and C. C. McIntyre, "Current steering to control the volume of tissue activated during deep brain stimulation," *Brain Stimul.*, vol. 1, no. 1, pp. 7–15, 2008.

[7] D. R. Merrill, M. Bikson, and J. G. R. Jefferys, "Electrical stimulation of excitable tissue: Design of efficacious and safe protocols," *J. Neurosci. Methods*, vol. 141, no. 2, pp. 171–198, 2005.

[8] J. P. Somann, G. O. Albors, K. V. Neihouser, K. H. Lu, Z. Liu, M. P. Ward, A. Durkes, J. P. Robinson, T. L. Powley, and P. P. Irazoqui, "Chronic cuffing of cervical vagus nerve inhibits efferent fiber integrity in rat model," *J. Neural Eng.*, vol. 15, no. 3, 2018.

[9] J. Wells, C. Kao, K. Mariappan, J. Albea, E. D. Jansen, P. Konrad, and A. Mahadevan-Jansen, "Optical stimulation of neural tissue in vivo," *Opt. Lett.*, vol. 30, no. 5, p. 504, Mar. 2005.

[10] A. D. Izzo, J. T. Walsh, H. Ralph, J. Webb, M. Bendett, J. Wells, and C.-P. Richter, "Laser stimulation of auditory neurons: effect of shorter pulse duration and penetration depth.," *Biophys. J.*, vol. 94, no. 8, pp. 3159–66, Apr. 2008.

[11] J. Wells, A. Mahadevan-Jansen, C. Chris Kao, P. Konrad, and E. Duco Jansen, "Transient Optical Nerve Stimulation," in *Neuroengineering*, 2007, pp. 21–1 – 21–19.

[12] E. S. Boyden, F. Zhang, E. Bamberg, G. Nagel, and K. Deisseroth, "Millisecond-timescale, genetically targeted optical control of neural activity.," *Nat. Neurosci.*, vol. 8, no. 9, pp. 1263–8, Sep. 2005.

[13] A. I. Matic, A. M. Robinson, H. K. Young, B. Badofsky, S. M. Rajguru, and C.-P. Richter, "Longterm infrared neural stimulation in the chronic implanted cat," in *Proc. SPIE 8565*, 2013, vol. 8565, p. 85655T–85655T–7.

[14] Q. Liu, M. J. Frerck, H. a. Holman, E. M. Jorgensen, and R. D. Rabbitt, "Exciting cell membranes with a blustering heat shock," *Biophys. J.*, vol. 106, no. 8, pp. 1570–1577, 2014.

[15] J. Wells, C. Kao, P. Konrad, T. Milner, J. Kim, A. Mahadevan-Jansen, and E. D. Jansen, "Biophysical mechanisms of transient optical stimulation of peripheral nerve.," *Biophys. J.*, vol. 93, no. 7, pp. 2567–80, Oct. 2007.

[16] S. L. Jacques, "Laser-Tissue Interactions: Photochemical, Photothermal, and Photomechanical," *Surg. Clin. North Am.*, vol. 72, no. 3, pp. 531–558, 1992.

[17] B. J. Raos, E. S. Graham, and C. P. Unsworth, "Nanosecond UV lasers stimulate transient Ca2+ elevations in human hNT astrocytes," *J. Neural Eng.*, vol. 14, no. 3, 2017.

[18] M. Wang, Q. Xia, F. Peng, B. Jiang, L. Chen, X. Wu, X. Zheng, X. Wang, T. Tian, and W. Hou, "Prolonged post-stimulation response induced by 980-nm infrared neural stimulation in the rat primary motor cortex," *Lasers Med. Sci.*, 2019.

[19] K. C. Stocking, A. L. Vazquez, and T. D. Y. Kozai, "Intracortical Neural Stimulation with Untethered, Ultrasmall Carbon Fiber Electrodes Mediated by the Photoelectric Effect," *IEEE Trans. Biomed. Eng.*, vol. 66, no. 8, pp. 2402–2412, 2019.

[20] H. Schmalbruch, "Fiber composition of the rat sciatic nerve," *Neuroanatomy*, vol. 215, no. 1, pp. 71–81, 1986.

[21] L. Yu, F. Nina-Paravecino, D. Kaeli, and Q. Fang, "Scalable and massively parallel Monte Carlo photon transport simulations for heterogeneous computing platforms," *J. Biomed. Opt.*, vol. 23, no. 01, p. 1, 2018.

[22] S. L. Jacques, "Optical Properties of Biological Tissues: A Review," *Phys. Med. Biol.*, vol. 58, no. 11, pp. R37–61, 2013.

[23] Y. Hoshi, Y. Tanikawa, E. Okada, H. Kawaguchi, M. Nemoto, K. Shimizu, T. Kodama, and M. Watanabe, "In situ estimation of optical properties of rat and monkey brains using femtosecond time-resolved measurements," *Sci. Rep.*, vol. 9, no. 1, 2019.

[24] S. A. Prahl, S. L. Keijzer, A. J. Jacques, and A. Welch, "A Monte Carlo Model of Light Propagation in Tissue," in *Dosimetry of Laser Radiation in Medicine and Biology*, G. Mueller and D. Sliney, Eds. 1989, pp. 102–111.

[25] M. J. Jou, S. Bin Jou, M. J. Guo, H. Y. Wu, and T. I. Peng, "Mitochondrial reactive oxygen species generation and calcium increase induced by visible light in astrocytes," *Ann. N. Y. Acad. Sci.*, vol. 1011, no. 5, pp. 45–56, 2004.

[26] V. Lumbreras, E. Bas, C. Gupta, and S. M. Rajguru, "Pulsed infrared radiation excites cultured neonatal spiral and vestibular ganglion neurons by modulating mitochondrial calcium cycling.," *J. Neurophysiol.*, vol. 112, no. 6, pp. 1246–55, Sep. 2014.

[27] A. M. Smith, M. C. Mancini, and S. Nie, "Bioimaging: Second window for in vivo imaging," *Nature Nanotechnology*, vol. 4, no. 11. pp. 710–711, 2009.

[28] C.-P. Richter, A. I. Matic, J. D. Wells, E. D. Jansen, and J. T. Walsh, "Neural stimulation with optical radiation.," *Laser Photon. Rev.*, vol. 5, no. 1, pp. 68–80, 2011.